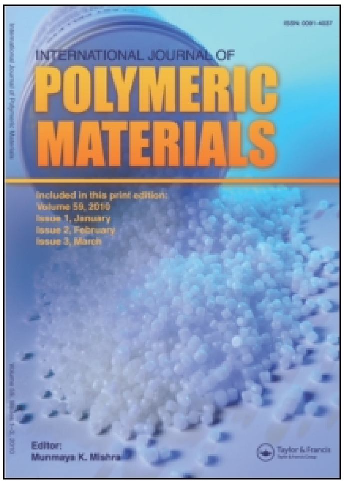

International Journal of Polymeric Materials
Publication details, including instructions for authors and subscription information:
http://www.informaworld.com/smpp/title~content=t713647664

Physical Properties of Polymer Solids and Control of Supermolecular Structure

Tisato Kajiyama[a]
[a] Department of Applied Chemistry, Faculty of Engineering, Kyushu University, Fukuoka, Japan

To cite this Article Kajiyama, Tisato(1991) 'Physical Properties of Polymer Solids and Control of Supermolecular Structure', International Journal of Polymeric Materials, 15: 3, 227 — 238

To link to this Article: DOI: 10.1080/00914039108041088

URL: http://dx.doi.org/10.1080/00914039108041088

Intern. J. Polymeric Mater., 1991, Vol. 15, pp. 227–238
Reprints available directly from the publisher
Photocopying permitted by license only

Printed in the United Kingdom

PHYSICAL PROPERTIES OF POLYMER SOLIDS AND CONTROL OF SUPERMOLECULAR STRUCTURE

TISATO KAJIYAMA

Department of Applied Chemistry, Faculty of Engineering, Kyushu University, Hakozaki, Higashi-ku, Fukuoka 812, Japan

1. Physical Properties of Polymer Solids

1. Superdrawing

Linear crystalline polymers can be processed to produce high degrees of orientation, sufficient to produce drastic increases in tensile strength and modulus. Ultra high modulus and strength fibers are produced from a high molecular weight polymer employing a variety of techniques, such as melt-spinning, super-drawing, solid-state extrusion, etc. Long polymer chains can be fairly well aligned and extended only after the polymeric chains are disentangled. Gel spinning is one of the preparation techniques of disentangled high molecular weight polymer with sufficient drawability.

Liu and Miyasaka (2375, E393) have investigated the effect of molecular weight distribution (MWDS) on the superdrawn structure and mechanical properties of ultrahigh molecular weight polyethylene (UHMW-PE). The effect of MWDS on the super-drawability and mechanical properties of UHMW-PE prepared by a solvent cast technique was investigated on the basis of tensile test and dynamic mechanical measurements. The superdrawn structure was characterized by thermoluminescence (TL), DSC and pulse NMR techniques. Two kinds of linear PE with approximately the same viscosity average molecular weight, Mv or 4.0×10^6 (average viscosity about 18.0) but different MWDS, (Mw/Mn) 3.0 and 5.0, were used. A xylene solution containing 0.4% g/100 ml of PE and 0.1% w/w of antioxidant di-butyl-p-cresol was prepared by heating a well blended/solvent mixture in a silicone oil bath at 150°C for about 2 hours. The sample cut from the dried gel film was clamped in a manually operated extender and drawn in a boiling water bath. The draw ratio was determined from the change in ink-marked distance after stretching. The TL from an x-ray irradiated UHMW-PE gel film was significantly affected by the treatment of ultra-drawing. The TL glow peak was correlated to the mechanical relaxation of the crystalline phase (the α_c - dispersion) in the UHMW–PE gel film. The TL integrated intensity is weak for folded-chain crystals but strong for extended-chain crystals. An extra higher TL peak was observed for the samples drawn up to 150x, which was related to the extended tie molecular chain regions in the ultradrawn film. The MWD makes a significant contribution to the ultra-drawability, and hence, to the ultimated mechanical properties, such as the magnitude of tensile modulus of the UHMW-PE cast films. The UHMW-PE having a narrower MWD(N-PE) reaches an ultimate structure at a lower draw ratio than the UHMW-PE having a broader MWD(B-PE), this effect being a result of the more extremely extended intercrystalline tie chains. It was also found that, at the same drawing temperature (100°C), N-PE showed a higher magnitude of modulus than B-PE at a draw ratio of up to 150x, which was the ultimate ratio for N-PE.

In the past few years, superdrawing of polyvinyl alcohol (PVA) has received increasing interest, since the tensile properties of PVA with a fairly high melting point (~250°C) in a crystalline state correspond to one of the highest among polymeric materials. Kiyooka and Kanamoto (2378, E394) studied the effect of initial morphologies such as gel and solution grown crystal (SGC) on drawability, as reflected in the resultant tensile and physical properties of the drawn PVA films. Gels were prepared by quenching a 2 wt% solution in mixtures of two good solvents: N,N-dimethyl formamide (DMF) and ethylene glycol (EG) at $T_{gel} = -70 \sim 80$°C. The prepared gel films were translucent before and after drying. SGC were precipitated isothermally at 50 ~ 130°C from a 0.1 wt% PVA solution in EG or triethylene glycol (tri-EG). These dried gel films and SGC mats showed the highest deformability by solid-state coextrusion followed by tensile drawing (two-stage drawing). Exudates exhibited strain-hardening during the second-stage tensile drawing at elevated temperatures. Drawability of gel films were markedly higher than that of SGC mats, and the gel, which were prepared under the following condition of DMF/EG = 1/1, $T_{gel} = -70$°C, showed the highest drawability, $Dr \leq 40$. The tensile properties of the drawn films at a given DR were not significantly affected by the initial morphologies such as SGC or gel, and increased with increasing DE. Thus, the tensile modulus and strength of drawn gel films reached to 70 GPa and 1.5 GPa, respectively, in the case of the highest achieved DR of 40. The peak melting point and the heat of fusion were also not significantly affected by the initial morphologies. The efficiency of drawing was estimated from the thermal elastic shrinkage. Molecular draw ratio (MDR), which corresponds to the deformation ratio of each molecular chain, was evaluated by the following equation, $MDR = ((L_t - L_s)/L_0) + 1$, where L_0, L_t and L_s are the length of a sample before and after drawing, and after shrinkage, respectively. For all drawn samples prepared from the gel films and SGC mats, MDR was nearly equal to DR, indicating that these films and mats were drawn highly effectively. They concluded that the gel films of PVA prepared from a mixed solvent of DMF/EF = 1/1 showed the highest drawability ($DR \leq 40$), and hence, the highest tensile properties (modulus ≤ 70 GPa and strength ≤ 1.5 GPa).

Takahashi and Okui (2384, E396) studied the formation mechanism of the fiber structure in a zone-drawing process and also, mechanical properties of the resultant fiber with special reference to the degree of crystallinity. They used polyethylene with molecular weight of about 1.5×10^5 and with molecular weight distribution, Mw/Mn of about 3 to 4. Highly-drawn polyethylene filaments were produced continuously by the zone-drawing method. The draw ratio could be controlled by altering the ratio of the feeding and take up speed. Young's modulus showed a better linear relationship with drawing stress than that with draw ratio. The crystallinity dependence of Young's modulus (E) and birefringence of amorphous phase, Δn_a can be divided into two crystallinity regions, the critical degree of crystallinity being about $0.7 \sim 0.8$. In a lower crystallinity region, the magnitude of E and Δn_a increase linearly but with only a slight increase in crystallinity. However these properties increase markedly with crystallinity, when the degree of crystallinity exceeds a critical value. It might be thought that the frequency or the probability of the crystalline block linkages is increased with an increase in the degree of crystallinity, and a remarkable increase in linkages of crystalline block beyond the critical crystallinity yields a marked increase in Young's modulus and birefringence of a amorphous phase.

2. Rigid and Heat Resistant Polymers

Low thermal expansion polyimides are very useful insulation films for many kinds of electronics applications, because they solve the problems in thermal stress due to a minimization of the thermal expansion coefficient mismatching between two or more materials.

Much effort has been exerted in the synthesis and characterization of polyimides. Excellent mechanical and thermal properties of some kinds of polyimides containing rigid chemical structure component have been recognized. Imidization conditions affect the morphology of polyimides. The change in morphology is anticipated to result in the observed property changes. Yamamoto and Etoh (2396, E400) investigated the effect of imidization conditions on properties of various kinds of homopolyimid. Copolyimides and polyimide blends containing p-phenylene pyromellitic imide moiety have also been studied. The polyimides were prepared by both conventional heating and a chemical method with an acetic acid anhydried/pyridine mixture, using monomers such as p-phenylene diamine, 4,4′-oxydianiline, pyromellitic anhydride, biphenyl tetracarboxylic acid anhydride and benzophenon tetracarboxylic acid anhydride. It has been shown that the mechanical and thermal properties of polyimides are strongly influenced by their imidization conditions. The densities of the polyimides obtained by the chemical method were lower than those by the heat method.

Epoxy resin has been widely used because of its excellent mechanical and electronic properties. When epoxy resin is cooled down from the curing temperature to room temperature, residual stress arises because of the difference in the thermal expansion coefficients of resin and substrate. The residual stress reduces the adhesive strength and induces cracks in the material. Nakamae and Nishino (2402, E402) used a X-ray diffraction method to detect the stress resided both at the interface between resin and substrate and in particulate composite materials. They epoxy resin used was one of a bisphenol-A diglycidylether type (Epikote 828) and 4,4'-diaminodiphenyl methane was used as the curing agent. They were mixed and cured (80°C, 2hrs or 180°C, 6 hrs) on aluminium plates (A1 plate). Strains in the (422) plane of the A1 plate were measured by X-ray diffraction. For the measurement of the residual stress in particulate composite materials, the (422) plane of A1 particle or the (331) plane of SiO_2, which were embedded in epoxy resin, were employed. By indicating the angle of incident the X-ray beams to the normal direction to the surface of the epoxy films, strain was measured at each incident angle of X-ray beam, ψ. When uniaxial stress is present, the relationship between ψ and ε can be expressed by the following equation,

$$\varepsilon = (1 + \nu)\sigma/E) \sin^2 \psi$$

where, E and ν are the elastic modulus and the poison ratio of each crystal, respectively. Using the $\sin^2 \psi$ method, σ was measured. When epoxy resin was cured on the A1 plate, the crystallite of the A1 plate was strained with a compressive residual stress of 30 MPa. On the other hand, the cured epoxy resin side was subjected to tensile residual stress. The residual stress, σ of the epoxy resin decreases with increasing aluminium filler content. Not only does the thermal expansion coefficient, β of the resin, but also the difference in β of the resin and substrate decreases by the incorporation of A1 particles and this is the reason why the magnitude of σ decreased. At the same time, the residual stress of substrate decreases with increasing filler content. Meanwhile, embedded particles were subjected to compressive stress when the epoxy resin was cured on poly(tetrafluoroethylene) plates. In this case, the difference in β of the resin and embedded particle causes the residual stress.

Etoh and Fukami (2399, E401) studied the dynamic mechanical properties for simultaneous interpenetrating polymer networks (SIN) prepared from the epoxy resin (DGEBA) cured with nadic methyl anhydride and 4,4'-dimaleimide diphenylmethane (BMI) — allylester copolymer. The allylesters were triallyltrimellitate (TAT), triallylisocyanurate (TAIC) and diallylisophthalate (DAP). The relative modulus in a rubber state starts to increase rapidly at a concentration of 30 ~ 40 wt% BMI-allylester, suggesting that the BMI-allylester copolymer becomes a mutual continuous phase at this concentration, Tg also increases rapidly and approaches an upper limiting value with increased loading of the EMI-allylester. The increase in Tg may arise from a combination of contributions arising from an increase in crosslink density and the effect of interactions between the epoxy resin and the BMI-allylester. The values of Tg can be correlated to the crosslink density ν by Tg = K_1, ln $K_2\nu$ where K_1 and K_2 are constants. Different asymtotic values of the Tg between each series of materials seem to result from the difference of chemical structure of each allylester. The value of the attractive component in the solubility parameter for each BMI-allylester approaches that of the epoxy resin in the order BMI-TAT, -TAIC and -DAP, coresponding to the asymptotic values of Tg. It became apparent from the Tg of each SIN analysed on the basis of the Fox & Loshaek equation that the maximum miscibility between the epoxy resin and the BMI-allylester copolymer occuring at a composition of 50%, being consistent with the results of density vs. composition.

3. Molecular Motion and Relaxation Phenomena

The secondary dispersion process pertaining to the local mode in the amorphous states have widely been observed for various materials and it has been reported that the intermolecular contribution to the local mode is more significant rather than the intramolecular one. In order to elucidate the intermolecular contributions to the secondary dispersion, Naoki and Hashizume (2363, E389) measured the pressure effects on the dielectric β process in comparatively simple molecular glasses, o-terphenyl (oTP) and triphenylchloromethane (TPCM), and also, two types of poly(vinyl chloride) (PVC) glass prepared under different pressures. The location of the β process in the time-temperature-pressure plane were represented by the frequency at the maximum dielectric loss, f_{max}. Also, the relaxation magnitude, $\Delta\varepsilon$ and the distribution of the relaxation time, $1-\alpha$ were determined from the Cole-Cole plot.Apparent macroscopic intermolecular contribution was obtained by adapting a simple thermally activation process. The magnitude of the relaxation time ($\sim\frac{1}{2}\pi$ f_{max}) can be determined from the average energy barrier, G*. The polarization of the solid in a region far from the critical point can be also evaluated from the average energy disparity induced by the electric field, ΔG. Then,

$$f_{max} \propto \exp(-G^*),\ \Delta\varepsilon \propto \exp(-\Delta G)$$

The magnitudes of P_iV^* and $P_i\Delta V$, (P_i, V^* and ΔV are the internal pressure, the activation volume and the volume disparity, respectively) correspond to those of energies required to produce V^* and ΔV inside the glass. By using the activation internal energy, E^* and the internal energy disparity, ΔE, which are equal to the enthalpy barrier and disparity corrected by the work done by the external pressure, respectively, themeasure of apparent intermolecular contribution can be evaluated as the ratios of P_iV^*/E and $P_i\Delta V/\Delta E$. the intermolecular contribution is about 10 percent to both the energy barrier and disparity for the PVC glass. The situation is very different for the molecular glasses of oTP and TPCM, i.e., the intermolecular contribution to the energy barrier is extremely small, but that to the energy disparity is larger than that for PVC. In the case of these molecular glasses, the main secondary relaxation mode may be attributed to the hindered vibrations revolving the molecular disks composed of the three phenyl groups.

The ultrasonic spectroscopy is a very convenient way to study molecular motions and the mechanical behaviour of amorphous polymers and can be observed over three decades in elastic moduli. Shirouzu and Matsushige (2414, E410) applied ultrasonic spectroscopy to measure molecular motions of polycarbonates from the glassy state to the melt state. BisA polycarbonates (PC) with three different molecular weight (Mw) and one modified polycarbonate with a methyl group to each benzene ring were investigated. Effective frequency range was limited to 2 ~ 5 MHz due to the ultrasonic characteristics of polyimid used as the buffer material in the measuring system. Ultrasonic attenuations were obtained as ratios of the detected and initial amplitudes. Attenuations start to increase near 150°C in the case of PC with higher Mw, corresponding to the start of the glass transition. Attenuation decreased beyond 190°C, suggesting the existence of a rubbery state. On the contrary, in the case of PC with lower Mw, attenuation started to increase rapidly at 192°C, suggesting direct transition to a molten state, i.e. absence of a rubbery state.

Yamanaka and Kaji (2426, E414) observed the difference in the molecular motion of polyepichlorohydrin (PECH) between bulk and polymer blend with polymethylmethacrylate (PMMA) by ^{13}C-NMR. PECH was found to be miscible with PMMA based on DSC measurement. The temperature dependence of the ^{13}C-NMR spectra (spin-lattice relaxation time (T1) and spin-spin relaxation time (T2) was measured. The blended PECH/PMMA sample was prepared by solvent casting from solution. Two kinds of solvent, toluene and THF were used to produce solutions with weight content of 60% PECH. The toluene cast film is transparent and has a single Tg, suggesting a compatible blend film. The THF cast film is opaque and shows two Tg, which corresponds to a phase separated state. ^{13}C-NMR spectra were recorded at 75 MHz with a VARIAN XL-300. ^{13}C-NMR spectra of PECH showed three peaks from chloromethylene, methylene and methine. The temperature dependence of the chloromethylene peak heights indicates that if PMMA chains existing near PECH chains they can inhibit molecular motions. The T1 minimum was observed at the lowest temperature (90°C) in the case of the bulk material and at the highest temperature (130°C) for the transparent blend. The greater shift of the temperature at the T1 minimum corresponds to greater restriction for the thermal molecular motion of PECH. The temperature dependence of the spin-spin relaxation time (T2) of PECH exhibited a peak at 140°C.T2 of methine carbon in the case of the transparent film is about 14 msec and that in the opaque film about 40 msec. The magnitude of T2 is more sensitive to a phase separated structure in the polymer blend than measurements of T1.

4. Fatigue Phenomena

The fatigue behaviour of polymeric engineering materials has received increasing attention to recent years. The elucidation of fatigue mechanism is one of the most important problems with respect to the selection criteria of engineering materials. In clarifying the fatigue characteristics of polymeric materials, it is important to investigate how the viscoelastic behaviour of polymeric materials under cyclic deformation influence the fatigue behaviour. Variation of the dynamic viscoelastic properties during the fatigue process reflect the change in the microstructure of polymeric materials. Heat due to the damping properties of the specimen can be generated during the fatigue process, however, little attempt has been made to elucidate fatigue behaviour from a standpoint of viscoelasticity.

Kaiya and Kajiyama (2351, E383) carried out fatigue tests of highly oriented high density polyethylene (HDPE) performed under the three different loading conditions of tension- compression, pure tension and pure compression cyclic strainings. Morphological observations revealed that the fatigue fracture behaviour depends on the type of cyclic deformation. In the case of cyclic straining including a compression component, the fracture surface is inclined by 45° to the direction of cyclic deformation. On the other hand, in the case of fatigue under tension the fracture surface was almost perpendicular to the direction of cyclic straining. The inclination of the fracture surface showed a strong relation to the kink-band formation along a direction of maximum shear stress. Froma surface temperature rise and the variation of dynamic viscoelasticity during fatigue process, a fatigue criterion based on hysteresis loss consumed for an internal structural change was established. The hysteresis loss for viscoelastic materials per unit volume and unit time under cyclic straining is given by equation (1).

$$H = \pi f \varepsilon_d^2 E'' \quad (1)$$

where f, ε_d, and E″ are frequency, strain amplitude and dynamic loss modulus, respectively. The hysteresis loss energy evaluated from equation (1) was divided into two parts, the energy disspated as a heat generation and that used for a structural change under cyclic straining. If the fraction of X from the total hysteresis loss energy is converted to heat, the heat generation, Q_+, is expressed as $X\pi f\varepsilon^2{}_d E''$. Also, the heat radiation, Q_-, is expressed as $\kappa\theta_s$, where κ and θ_s are the heat transfer coefficient and the degree of temperature rise, respectively. Surface temperature rise is then expressed as follows:

$$d\theta_s/dt = (Q_+ - Q_-)/\rho c = (\kappa\pi f\varepsilon^2_d E'' - \kappa\theta_s)/\rho c \tag{2}$$

where ρ and c are density and heat capacity, respectively. Equation (3) was used to evaluate the constant value of k from the variation of specimen temperature after fatigue failure.

$$d\theta_s/dt = — \kappa\theta_s/\rho c \tag{3}$$

The magnitude of k was evaluated to be 44 $kJm^{-3}K^{-1}s^{-1}$. In order to discuss the relationship between the magnitudes of χ and fatigue lifetime, the average value of χ during fatigue process, χ was evaluated from the following equation.

$$\bar{\chi} = \int_0^{t_f} \chi dt/t_f \tag{4}$$

The magnitude of $1-\bar{\chi}$ increased with decreasing fatigue lifetime. This clearly indicates that a reduction in the ratio of heat generation to the total hysteresis loss energy leads to shorter fatigue lifetime. The averaged hysteresis loss, H_{av} during cyclic fatigue was evaluated as follows.

$$H_{av} = \int_0^{t_f} (1-\bar{\chi}) H dt/t_f \tag{5}$$

The slope of this logarithmic plot of H_{av} vs. t_f is -1 in a short fatigue lifetime region. The magnitude of H_{av} approaches a certain magnitude, H_O in a fairly long fatigue lifetime region. Therefore, the empirical relationship between H_{av} and t_f can be represented by equation (6) as the fatigue criterion which is similar to that proposed for unoriented polymeric specimens.

$$(H_{av} - H_o)t_f = C \tag{6}$$

where C is total hysteresis loss up to a fatigue failure. Equation (6) means that fatigue failure occurs when the effective hysteresis loss energy, $(H_{av}-H_o)t_f$ reaches a certain magnitude, C. At the same fatigue lifetime, H_{av} for tension-compression type cyclic straining is smaller than those for the other two types of cyclic straining. This indicates an ease of crack propagation due to induced kink-band formation. In the case of a compression type fatigue test, the fatigue lifetime is longer than that for tension-compression type fatigue for similar cases at the same magnitudes of H_{av}, since crazes generated in the kink-band boundary are compressed, eliminating the absorption of energy due to cyclic straining.

2. Control of Supermolecular Structure

Aggregation Structure in Membrane

Kamide and Iijima (2441, E419) investigated the effect of preparation conditions on supermolecular structure of a cellulose micro-porous membrane. According to the particle growth theory proposed by them, the polymer-rich phase or the polymer-lead phase separates initially from the solution depending on the initial polymer concentration, $V_P{}^o$ is smaller than the critical solution concentration, $V_P{}^c$ ($V_P{}^o < V_P{}^c$), the polymer-rich phase separates as primary particles, growing into the scondary particles to form network structure in the membrane. If $V_P{}^o$ is larger than $V_P{}^c$ ($V_P{}^o > V_P{}^c$), the polymer-lean phase separates as particles and circular pores are formed in the membrane. An attempt was made using the micro-porous cellulose membrane prepared by the micro-phase separation method; (1) to determine the cloud point curve and critical point of a quasi-ternary system of cuprammonium cellulose/acetone/water, (2) to estimate the pre shape, diameter of the secondary particles, $2S_2$ and mean pore diameter, $2r_o$ by electron microscope and also, (3) to establish the relation between pore characteristics of the membrane which has network structure on its front surface and its preparation conditions. The casting solution is thought to be phase separated at the critical point, when acetone is used as coagulation solution ca. 65wt%. Membranes were prepared by two methods; a cellulose solution was cast on a glass plate, and then, (a) immersed into a coagulation solution which contains acetone (30, 40, 50, 70 and 90 wt%), ammonia (0.56 wt%) and water (the liquid method), or (b) placed in a gaseous phase of acetone (the gas method). With the membranes were prepared from a 7.0 wt% cellulose solution by the liquid method, the front surface were constructed by secondary particles forming a network structure when acetone concentrations are 30 and 40 wt%, i.e., $V_P{}^o < V_P{}^c$, but the network structure became vague at acetone concentration of 50 wt%. It was difficult to decide pore shape on the front surface of the membranes prepared with 70 and 90 wt% acetone by electron micrographs at a magnification of 30,000. The membranes prepared from a 8.0 wt% cellulose solution by the gas method in condition of $V_P{}^o > V_P{}^c$, have circular pores on their front surfaces. The diameter of the pores grew bigger during the progress of phase separation. With an increase of cellulose concentration in the casting solution, $2S_2$ on the front surfaces of the membranes prepared by the liquid method decreased. $2r_o$ of the front surfaces were in proportion to $2S_2$.

Ishizu and Fukutomi (2435, E417) established a preparation method for vertically-oriented microdomains of block and graft copolymers or polymer blends by means of epitaxial growth of a microdomain pattern on the surface of a supported film. Their first aim is to describe the control of the microdomain structure (horizontally-oriented lamellar and cylindrical domains) of poly(styrene(S)-b-isoprene(I) diblock copolymers by means of segment absorptions from the surface of crosslinked PS as a support film. The second aim was to prepare the vertically-oriented microdomain patterns of greater thickness using polymer blends showing miscibility windows. The well-defined poly(S-b-I)(Mn $= 5.7 \times 104$, PS 0.60 wt frac.) was prepared by sequential anionic addition. The composite films were fabricated by casting (S-b-I) block copolymer solutions in benzene or cyclohexane, on a surface of crosslinked PS as a support film. The cross section of the composite film specimens was observed by transmission electron microscopy. Near the boundary surface of PS networks, the onion-skin morphology of PS/PI lamellae was aligned with their interfaces parallel to the matrix of PS networks, generating this structure for several layers. On the other hand, at the free surface of the upper layer, the alternating lamellar structures of PI/PS microphases were oriented horizontally to the surface which contracts with air. A composite film was prepared by casting a blend of poly (4-vinylpyridine)(P4VP) and S/acrylonitrile (AN) random copolymer (AN, 17.6 mol%) on the surface of domain-fixed poly-(S-b-4VP) block copolymer film. It was found from SEM micrographs that S/AN copolymer/P4VP blend formed microphase-separated structures by epitaxial growth. The thickness of obliquely oriented microdomains of blend was about 13μm as judged from electron micrographs.

Morphology Control of Rigid Polymers

Yamashita and Kato (2444,E420) reported that poly(p-oxybenzoyl) (POB) whiskers were obtained during polymerization of p-acetoxybenzoic acid in liquid paraffin. The formation mechanism of the whiskers has been suggested as follows; (1) Oligomers of low degree of polymerization are formed in a homogeneous polymerization, and as soon as the degree of polymerization exceeds a critical value, oligomeric materials crystalline in the form of lamellae from the solution. If the slip dislocation is formed in the precipitated lamellae, subsequent crystallization occurs at the slip plane rather than at the usual growth plane because of the advantage of the secondary nucleation for crystal growth. (2) The degree of polymerization increases by transesterification in the interlamellar regions, and reorganization of crystals occurs. To control the morphology of rigid polymers by this preparative method, the features of crystal growth in the polymerization system, in which crystallizable materials are continuously produced, should be understood. The shape change of POB whisker for various polymerization time was studied in more detail. The length and the diameter of whiskers and the angles of both pointed ends of whiskers were measured as a function of polymerization time. The average length with sharp distribution increases with increasing polymerization time. From this fact, the lamellar crystals with slip dislocation which causes the spiral growth seem to be formed only at the very early stage of polymerization. Subsequently crystallizable oligomeric materials are exhausted only in the crystal growth. In the first step of whiskers growth, the increase of the diameter are also observed to be accompanied by increase in length. This is due to the high degree of supersaturation of crystallizable materials. In the intermediate step, the increase in length only occurs. In the final step, the angles of both pointed ends of whiskers become sharper. This is due to the change of nucleation controlled growth mechanism to diffusion control. The number of crystals was estimated from the amount of the precipitated material and the average volume of crystals at each polymerization time. It did not change in the course of the polymerization. This fact also confirmed the observation that the incipient crystals of whiskers are formed only at the very early stage of polymerization. It was concluded that the shape of change of POB whiskers was explained by the effects of the degree of supersaturation of the crystallizable oligomeric materials in paraffin.

3. Polymer/(Liquid Crystal) Composite System

Liquid crystalline (LC) materials for a display are utilized in a cell sandwiched between conducting glass plates because of the low viscous fluid nature of the materials. However, the geometrical shape of the device is fairly restricted in fabricating such a glass cell. Polymer/LC composite film, in which a continuous LC phase is embedded in a three dimensional network of polymer matrix, is a stable self-supported LC film in spite of its very low viscous character. Therefore, the functional characteristics of LC can be developed as a self-supported flexible LC film which are ultrathin and have a large area. The self-supported LC films have been investigated as unique and novel permselective membranes for molecular filtration, oxygen enrichment, photoresponsible active and facilitated transport of metal cation and so on. The self-supported LC film can be expected to be useful as a very large area light-controllable film (light valve) or information displays.

Kajiyama and Kikuchi (2450, E422) investigated electro-optical properties of polymer/(liquid crystal) composite films based on light scattering controlled by an a.c. electric field. Scanning electron microscopic observation for the matrix polymer after extraction of LC with methanol indicated that the LC molecules were continuously embedded in a three-dimensional spongy network of polymer. Such a membrane system with many optical interfaces plays an important role on light scattering in the absence of an imposed electric field. A high contrast of light-switching was observed; 3% transmittance of the as-cast composite film changed to 81% transmittance with the response time of 0.3 ms in the case of an applied 250 V_{P-P} a.c. electric field of 10 kHz at 333K.

Thermotropic liqud crystalline polymers with mesogenic side chain groups have both characteristics of polymers and liquid crystals. Recently, electro-optical properties of thermotropic liquid crystalline polymers have been studied extensively. However, in a mesomorphic state the liquid crystalline polymer (LCP) are more viscous than low molecular weight liquid crystals (LMWLC). Therefore the magnitude of the response time of LCP's are much greater than for the equivalent LMWLC molecules due to their remarkably high viscosity in a mesomorphic state of the LCP. Kajiyama and Moritomi (2453, E423) prepared composite systems composed of side chain type LCP and LMWLC whose chemical structure is similar to the mesogenic side chain. The aggregation state, phase transition behaviour and electro-optical effect of these composite systems were investigated. Poly(4-cyanophenyl 4′-propyloxy benzoate methyl siloxane (PCPPS) or poly(4-cyanophenyl 4′-hexyloxy benzoate methyl siloxane) (PCPHS) was used as LCP and 4-cyanaophenyl 4′-hexyloxy benzoate (CPHOB) was used as LMWLC. The phase transition behaviour and the aggregation states of the PCPHS/CPHOB and PCPPS/CPHOB composites were investigated on the basis of DSC measurement, polarizing optical microscopic observation and X-ray diffraction study. The electro-optical effect of these materials was evaluated using an applied a.c. electric field.The composites form the phase-separated structures below T_{km} for CPHOB, but CPHOB is misible over the whole range of concentration with PCPPS and PCPHS in the isotropic and mesophase phases. Application of a low frequency a.c. electric field induces a high light scattering state of the composites due to turbulent flow caused by an ionic current. On the other hand, under a high frequency electric field, a non-scattering (transparent) state was produced from a homeotropic alignment. A high contrast electro-optical effect was produced by using these reversible bistable phenomena and these high or non-light scattering states were stored in the smectic phase with a rise time of the order of several hundreds msec.